ejpmr, 2016,3(6), 50-55

SJIF Impact Factor 3.628

EUROPEAN JOURNAL OF PHARMACEUTICAL AND MEDICAL RESEARCH
www.ejpmr.com

Research Article
ISSN 2394-3211
EJPMR

CHARACTERISING SENSITIVE SUBMICRO-BI-HALL PROBE SENSORS OF LIFT-OFF TECHNIQUES FOR APPLICATIONS IN SCANNING HALL PROBE MICROSCOPY(SHPM)

Hussein Ali Mohammed and Ayoub Abdulwahid Bazzaz*

Department of Basic Sciences, Faculty of Dentistry, University of Kerkuk, Kerkuk, Iraq.

***Corresponding Author: Dr. Ayoub Bazzaz (BSc,MSc,PhD,DPSI)**
Department of Basic Sciences, Faculty of Dentistry, University of Kerkuk, Kerkuk, Iraq.

Article Received on 28/03/2016 Article Revised on 18/04/2016 Article Accepted on 08/05/2016

ABSTRACT
Bismuth Hall (Bi-Hall) sensors with an active size range of (75nm-2μm) manufactured by electron beam lithography and lift-off techniques for applications in scanning Hall probe microscopy(SHPM) were systematically characterised for functional device size. Using higher Hall probe currents the miniumum detectable field of 100nm probes, at room temperature and dc currents of 5A is found to be B_{min}=0.9mT/Hz$^{0.5}$ with a scope of >10 reduction factor. This is significantly lower than those in similar samples manufactured by focussed ion beam (FIB) milling of continuous Bi films. Our finding suggests that the elimination of FIB damage and Ga^+ ion incorporation through the use of lift-off techniques could produce superior figures of merit. Further ways in which the 300K performance of our sensors could be improved too.

KEYWORDS: Sub-micro-Bi-Hall probe, lift-off techniques, scanning Hall probe microscopy.

INTRODUCTION

Magnetic Force Microscopy (MFM) is currently the accepted tool in the data storage industry for characterising the nano-scale magnetisation distribution in ferromagnetic media, particularly ferromagnetic domains and domain walls.[1,2] The magnetic force microscopy (MFM) is a scanning probe technique that measures the force between an oscillating magnetically-coated tip and the sample, does suffer from two characteristic weaknesses. Firstly, the sharp magnetic tip is invasive and can perturb the magnetic structure of the sample (or vice versa); secondly, the micro-magnetic structure of the tip is rarely known with any confidence, rendering imaging results qualitative rather than quantitative in most cases. Consequently there is a key outstanding requirement for a quantitative and non-invasive imaging technique to complement MFM. Moreover, this new technique must operate effectively at room temperature, since it is generally undesirable to cool ferromagnetic sample cryogenically for characterisation. One promising candidate technique is scanning Hall probe microscopy (SHPM).[3] Although the latter has been widely used for investigating flux structures in superconductors at low temperatures; however, it has not been extensively used at 300K, due to the typically poor minimum detectable fields at room temperature. As a result, the current developments in SHPM are focusing on designing and manufacturing novel nanoscale Hall sensors with lower noise convenient for use at 300K.

High spatial resolution requires the sensors of SHPM to be manufactured with nanoscale dimensions and to operate in close proximity to the sample surface. However, high magnetic field resolution needs a large Hall coefficient (low carrier density), and low Johnson and 1/f noise. In addition low offset resistances are highly desirable, preventing saturation in high gain and low noise preamplifiers. These criteria are all well satisfied in GaAs/AlGaAs heterostructure two dimensional electron gases (2DEGs) at low temperatures, when they have very high carrier mobility.[4] Sensors with dimensions down to ~100nm have been demonstrated and 2DEGs typically have low carrier concentration and are confined close to the surface of the chip.[5] Nevertheless, at room temperature, the much lower carrier mobility leads to much higher lead resistances and Johnson noise, and dramatically increased minimum detectable fields.[6] Low frequency of 1/f noise increases rapidly at low Hall currents, further degrading minimum detectable fields. Other III-V semiconductor materials have been investigated with a view in achieving superior 300K performance, including InSb thin films[7,8], InAs/GaSb[9,10] and InGaAs/AlGaAs[11] quantum wells. Although some improved figures of merit have already been demonstrated in these alternative semiconductor systems at room temperature, all do show some associated limitations.

In practice, at room temperature, the semimetal Bi-Hall sensors prove to be superior to low carrier density semiconductor systems, due to their higher Hall probe currents and lower lead resistances which outweigh the disadvantage of a considerably lower Hall coefficient. Thin Bi films have the disadvantage that the carrier concentration depends quite strongly on a number of factors e.g. substrate material, deposition technique and film thickness.[12] Scanning Bi-Hall probe sensors have already been widely[13,14] and nanoscale devices with active sizes down to ~50 nm and recognised by focussed ion beam (FIB) milling of larger thin film structures.[8,15,16] However, it was found that devices smaller than 40nm were not operational, presumably due to damage and Ga+ ion incorporation during FIB.[15] These effects can be expected to increase device resistances and noise levels, and suggest that alternative manufacturing methods could lead to improved figures of merit. Recently the use of lift-off techniques was demonstrated for fabricating low noise static nanoscale Bi-Hall sensors for monitoring domain wall motion.[17] This work was extended here to investigate the use of electron beam lithography and lift-off to fabricate scanning submicron Bi-Hall sensors. Sensors were systematically studied as a function of Bi film thickness and active dimensions in the range 75nm-2μm, and the key figures-of-merit for our devices are reported below.

MATERIALS AND METHODS

Sub-micron thin film Bi-Hall effect sensors have been fabricated by optical and electron beam lithography and lift-off on semi-insulating GaAs substrates. Bismuth was selected for the active Hall element of our devices as at room temperature, it has a low carrier density and relatively high carrier mobility. Two different Bi film thicknesses (40 nm and 60 nm) were compared with the goal of optimising the sensor signal-to-noise ratio by exploiting the well-known dependence of the carrier density on thickness.[18]

A semi-insulating GaAs wafer was diced into 6.0mm x 6.0mm square chips and four Hall sensors prepared on each chip, one in each quadrant. Cr(20nm)/Au(200nm) Ohmic contacts were first patterned by optical lithography, thermal evaporation and lift-off in acetone. These chips were then cleaned in an ultrasonic bath rang around (20-25%) power for 15 minutes in solutions of trichloroethylene, acetone and isopropanol respectively. They were then dried using high pressure nitrogen gas and put in a Petri dish. This process avoids contamination in keeping everything perfectly clean so that the best chips are obtained. The clean chips are stuck on glass slides (22mm 22mm) cover slips (rotated at a 45° angle to spread the resist to the corner of the chip using photo resist (Shipley Microposit) S1813 with the active side facing up and then baked at 90oC for 30 minutes. The purpose of this step was to ease control on the chips during the lift-off fabrication process without scratching them with a pair of tweezers. Sticks chips with a glass slide to be used. These were made ready for the next a step which was the spinning process where spin on S1813 resist at 500 rpm for 5 seconds and 5000 rpm for 45 seconds and then baked in oven at 90oC for 15 mints. This is done to facilitate ease of handling during deposition processes. The samples are soaked in fresh chlorobenzene for 4 minutes so as to make the top layer hard by removing the solvent from it. Should the resist start turning bring pink, immersion time was reduced to 2 minutes. The next step was returning them to the oven to bake for the same time and temperature for 15 minutes, 90oC respectively. Lumps of 99.99% purity Bi were etched in concentrated HCl:H2O (1:5) to strip surface oxides and loaded into a Tungsten boat in a thermal evaporator. After pumping down, the samples were cleaned for 5 minutes in an Ar plasma and coated with 40 nm or 60nm Bi films at a deposition rate of 0.25–0.5nm/s, monitored with a quartz crystal thickness monitor. Hall probes based on wire-width in the range 75nm-2 μm were then identified by lift-off in hot acetone in an ultrasonic bath. Contact resistances measured at this stage of fabrication were found to be unacceptably high (>750kΩ). To rectify this a second Cr(10nm)/Au(50nm) metallisation was evaporated on top of the Bi leads, after which contact resistances were found to be very low (<10Ω). Typically, two terminal resistances of completed sensors lie in the range 1-4 kΩ at room temperature. SEM images of a 75nm wire width sensor manufactured in a 50nm thick Bi film are shown in figure 1.

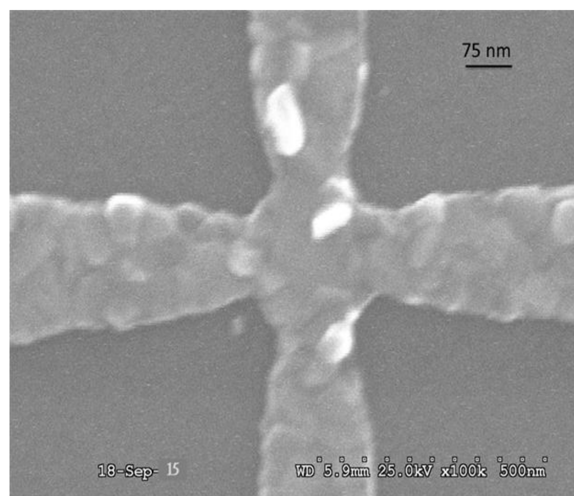

(Fig. 1): SEM image at two different magnifications of a 40nm thick Bi-Hall probe based on the intersection of two 75nm width wires.

The completed chips were glued with epoxy onto 0.5mm thick 10mm×10mm alumina packages. These were coated with gold leads which were wire bonded to the contacts on the chip with 25μm Au wire. Long Cu wires were then Indium soldered to the leads on the package, for connection to terminals on the sample holder. The latter was the insert for a variable temperature cryostat and had 16 terminals on the sample plate connected by twisted pairs of Cu wires to BNC connectors in a connection box on top. The sample rod was inserted into

the static sample space of a cryostat, evacuated and back-filled with Helium gas to prevent oxidation or other degradation of the Bi probes during characterisation. The tail of the cryostat containing the sample sits in the middle of a commercial electromagnet capable of generating a maximum field of ~100mT perpendicular to the plane of the sample. The electromagnet was driven by a bipolar power supply, allowing the magnetic field at the Hall sensor to be smoothly varied and reversed. In order to characterise the Hall coefficient, sensors were driven with a 1-10 µA 32Hz ac current from a commercial function generator in series with a 1MΩ resistor. The Hall voltage and offset voltage were detected with a Stanford Research Systems SR830 digital lock-in amplifier. The sensor noise was characterised using a home-made batterydriven programmable dc current source and ultra-low noise preamplifier with 104 gain. Noise spectra were then measured in the range 0-100Hz at fixed Hall currents with a Hewlett-Packard HP3561A dynamic signal analyzer. One hundred individual noise spectra were automatically averaged in the DSA to build the datasets presented below.

RESULTS

In figure 2 the Hall coefficients measured at room temperature for a large number of Hall probes with wire widths (75nm - 2 µm) and a 10 µA Hall current, with sensors manufactured in both 40nm (stars) and 60nm (circles) thick Bi Films. The initial results showed consistency with the expectation that the Hall coefficient is constant for a given Bi thickness. However, a rather large fluctuations around the mean was detected in each case by a horizontal dashed line. The latter is smaller for the 60nm probes (RH(60nm) ≅1.98Ω/T) than the 40nm probes(RH{40 nm}≅2.95Ω/T). The large fluctuations detected from probe to probe are almost certainly linkable to rather random granularity of the Bi films. The grain structure in 60nm films appears to be somewhat coarser than in the 40nm ones is attributable to the largest fluctuations in these sensors.

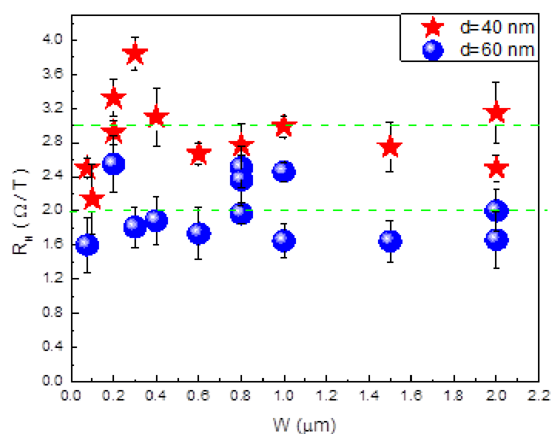

(Fig. 2): Measured room temperature Hall coefficient as a function of cross wire width for probes manufactured in 40 nm (stars) and 60 nm (circles) thick Bi films.

Ironically, a Hall sensor should show a zero Hall voltage when the external magnetic field is zero; however, the performance of Hall effect sensors can be limited by offset resistances arising from misalignment of Hall voltage contacts or spatially inhomogeneous current flow in the Hall probe itself. It is important to keep the generating offset voltages to a minimum, as they can limit the gain and fidelity of the pre-amplification stage used in the detection scheme. The offset resistance defined as $R_{off} = V_H(H=0)/I_H$, where V_H(H=0) is the Hall voltage at zero magnetic field and I_H is the Hall probe current (Fig. 3). A very large spread in the distribution of offset resistances, were found in the 60nm thick samples generally being larger than those of 40nm samples, which is attributed to the a random granular structure of the films. In the smallest sensors the width of the active area is a bit larger than the grain size, and inhomogeneous current flow through grains while grain boundaries could be expected. For optimised structures, however, the offset resistance can be as low as ~0.1Ω, which correspond to an effective field of about 50-100mT.

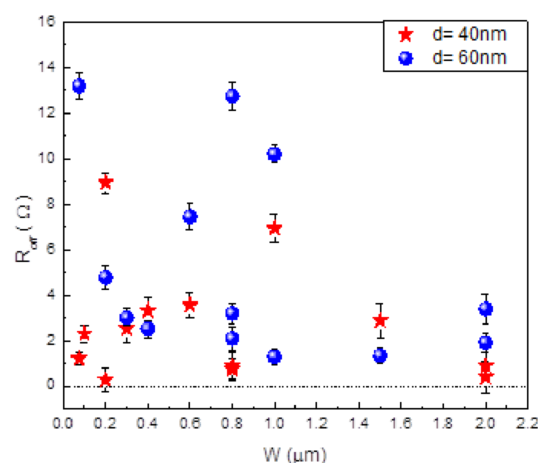

(Fig. 3): The measured room temperature offset resistances as a function of cross wire width in 40nm (stars) and 60nm (circles) thick Bi films.

Ironically, a Hall sensor should show a zero Hall voltage when the external magnetic field is zero; however, the performance of Hall effect sensors can be limited by offset resistances arising from misalignment of Hall voltage contacts or spatially inhomogeneous current flow in the Hall probe itself. It is important to keep the generating offset voltages to a minimum, as they can limit the gain and fidelity of the pre-amplification stage used in the detection scheme. The offset resistance defined as *Roff* □ *VH*(*H* □ 0) *IH* , where VH(H=0) is the Hall voltage at zero magnetic field and IH is the Hall probe current (Fig. 3). A very large spread in the distribution of offset resistances, were found in the 60nm thick samples generally being larger than those of 40nm samples, which is attributed to the a random granular structure of the films. In the smallest sensors the width of the active area is a bit larger than the grain size, and

inhomogeneous current flow through grains while grain boundaries could be expected. For optimized structures, however, the offset resistance can be as low as ~0.1Ω, which correspond to an effective field of about 50-100mT. The signal-to-noise ratio (SNR) of our Hall sensors is limited by their frequency-dependent noise voltage, $V_n(f)$. At high frequencies, above the 1/f noise corner, this is governed by thermal Johnson noise, V_J.[3]

$$V_J = \sqrt{4R_V k_B T \Delta f} \text{ .... } (1)$$

where R_V is the resistance between the voltage leads, k_B is the Boltzmann constant, T is the temperature and Δf, the measurement band width. At low frequencies the spectrum is dominated by 1/f noise that has a wide range of possible origins, such as carrier fluctuations due to trapping/de-trapping at defects or electron-hole generation-recombination processes.[19] The amplitude of the 1/f noise and the location of the 1/f noise corner increase quite rapidly as the sensor current increases.

Typical noise spectra, at three different Hall currents for a 0.3um wire width sensor manufactured in a 40nm Bi film are captured with a preamplifier gain of $G=10^4$ (Fig.4). The horizontal dashed line indicates the high frequency Johnson noise floor, corresponding to a voltage lead pair resistance of 3.1 kΩ, close to the value of 3.4 kΩ measured independently. The low frequency noise grew rapidly with Hall current and the 1/f shoulder simultaneously shifts to higher frequency, rising above the expected range of measurement frequencies at I_H=47uA.

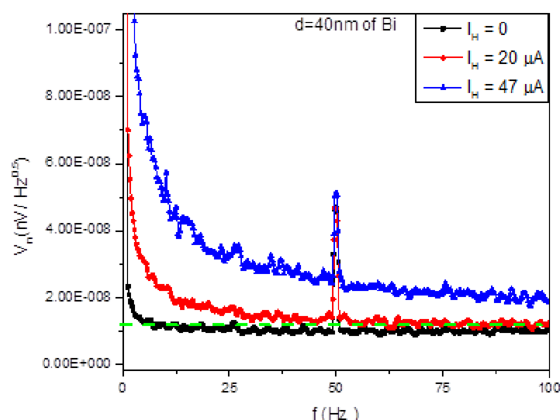

(Fig. 4): The noise spectral density at room temperature, V_n, as a function of measurement frequency for a 0.3um wire width Hall sensor patterned in a 40nm Bi film at three Hall probe currents. The horizontal dashed line indicates the high frequency Johnson noise floor.

One of the most useful figures of merit for a Hall sensor is the minimum detectable field, B_{min}, defined by the magnetic field at which the Hall voltage equals the noise voltage. At frequencies above the 1/f noise corner this can be approximated by:

$$B_{min} = \frac{\sqrt{4R_V k_B T \Delta f}}{I_H R_H} \text{ ....(2)}$$

The minimum detectable field plotted as function of Hall cross wire width for various measurement currents, patterning smaller Hall probes leads to a rapid increase in the minimum detectable field, due to their higher current densities for comparable Hall currents, and hence larger 1/f noise (Fig. 5). Optimal Hall probes with wire widths ≥1 um are found to have minimum detectable fields ~0.1mT/$Hz^{0.5}$ for Hall currents >70uA, while deep sub-micron probes have values in the range of 0.1-1 mT/$Hz^{0.5}$ for Hall currents in the range 5-20uA.

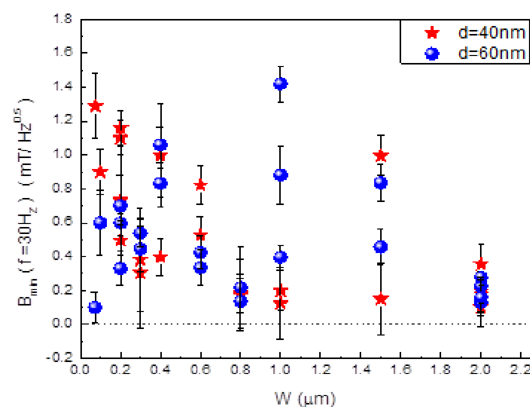

(Fig. 5): Room temperature minimum detectable fields (f=30Hz) as a function of cross wire width for probes in 40nm (stars) and 60nm (circles) thick Bi-films.

DISCUSSION

It is well established fact that the Hall coefficient of Bi-thin films is a strong function of the substrate material, film thickness and deposition method/conditions.[20] The average Hall coefficients of 2.95Ω/T(1.98Ω/T) measured in sensors in 40nm(60nm) thick Bi-films compares reasonably well with similar samples reported in the literature. The R_H=4.0 Ω/T in a 50nm probe milled by FIB in a 60nm Bi-film deposited on semi-insulating GaAs.[8] Such a somewhat larger value could have arisen as a consequence of the much more rapid evaporation rate (~10 x faster) used to grow their Bi-films, leading to a finer grain size and the loss of more free carriers to surface traps. The R_H=1.73 Ω/T in a 750nm probe FIB milled in a 78nm thick Bi-film grown on an oxidized Si-substrate.[15] This is much closer to typical values measured in our sensors and any difference can probably be attributed to the different choice of substrate. The reduction of Hall coefficient with increasing current was attributable to an increase in the sensor temperature combined with a negative temperature coefficient for $R_H(T)$. Publications reporting values for typical offset resistances are scanty. However, the recent value of 26.6 Ω in 40nm wide probes FIB milled into a 50nm thick Bi film of Petit and coworkers[16] is substantially larger than we typically measured in our smallest sensors, suggesting that FIB-milling might significantly increase current inhomogeneity in such small devices.

Some authors had presented estimates based only on Johnson noise corresponding to measurement frequency limit which is well above the 1/f noise corner. This however, is significantly underestimates the true noise level at lower frequencies. The minimum detectable fields at room temperature of our smallest Hall probe sensors is comparable with similar sized devices reported in the literature. This seems to be somehow a complicated process. Adopting this approach initially, the high frequency minimum detectable fields for our 100nm sensors are ~10-80µT/$Hz^{0.5}$ for Hall currents in the range 5-40µA. This is reasonably consistent with 70µT/$Hz^{0.5}$ in the 50nm Bi probes of Sandhu and coworkers[8] and with 5.1µT/$Hz^{0.5}$ for the larger 750nm Bi probes of Petit and coworkers.[16] Other reports implied B_{min}~10µT/$Hz^{0.5}$ for the 0.8µm GaAs/AlGaAs sensors[6], 0.72µT/$Hz^{0.5}$ for the 500nm InSb sensors of other scientists[7,8]], 0.5µT/$Hz^{0.5}$ in the 5µm GaSb/InSb probes of Grigorenko co-workers[9] and of Kazakova, coworkers[10] and 0.4µT/$Hz^{0.5}$ in the 2µm $In_{0.15}Ga_{0.85}As$ quantum well sensors of Pross, coworkers.[11] Since most of these devices are considerably larger than the smallest Bi probes measured here, the lower noise levels are not surprising. The noise figures for the 500nm structures of Sandhu, coworkers[8] are impressive, but the growth of epitaxial InSb thin films remains a major challenge, nor is clear enough the possibility of reducing the size of these devices.

A more realistic estimate of minimum detectable fields is obtained by directly measuring the spectral noise density at typical operation frequencies. Our data focus on the noise at 30 Hz, since this is the typical detection frequency used to operate our sensors. We also assume that the noise spectrum with such a low frequency ac current approximates to that with a dc drive of the same mean density. For our 100nm sensors designed from a 40nm Bi film does yiled an upper bound of B_{min}=0.9mT/$Hz^{0.5}$ with a 5µA Hall current. However, in order to avoid sensor damage the current density has been kept low and the optimal drive current is probably up to ten times larger. Using larger currents in 200nm and 300nm sensors the measured minimum detectable field have dropped to 0.5mT/$Hz^{0.5}$ and 0.3mT/$Hz^{0.5}$, respectively. The measured noise spectra as a function of size for probes FIB milled from 78nm Bi films for a 100 nm probe, a value of B_{min}(30Hz)~2 mT/$Hz^{0.5}$[15] could well be interpolated. This is significantly higher than in our somewhat thinner EBL sensors, possibly due to FIB induced damage and/or Ga^+ ion incorporation. All comparisons with equivalent sized Bi Hall probes reveal that our best probes exhibit similar or better minimum detectable fields in all cases. Other scientists have reported different outcomes for optimum values for their measurements.[5,9,10]

Clearly the optimal minimum detectable fields for these alternative materials systems are somewhat lower than our Bi sensors, however, these data are for devices that are typically more than an order of magnitude larger than those we have studied here. Hence these semiconductor devices do not provide a comparable benchmark and in some cases it is not clear if their sizes could be reduced to deep sub-micron dimensions. The noise levels of our devices are lower than those reported for otherwise comparable FIB milled sensors. This suggests the likelihood consequence of the elimination of FIB damage and Ga^+ ion incorporation through use of lift-off techniques does indeed lead to superior figures of merit in these Bi sensors.

There is still much ahead that could be done to optimise the figures of merit of Bi Hall effect sensors. Recently, Kubota and co-workers[17] have used advanced electron beam lithography and lift-off techniques to manufacture static 40nm Hall probes in a 75nm Bi film. The much thicker film yields lower lead resistances and allows much higher Hall currents to be used, reported values of B_{min}~0.012mT/$Hz^{0.5}$ at a frequency of 1000Hz. The same approach could be used to optimise scanning sensors, although there is a price to pay in spatial resolution, since the local magnetic induction can no longer be assumed to be uniform throughout the depth of the film. A much more comprehensive study of the noise spectra, as a function of Hall current, is required to optimise sensor performance. In practice the increase in 1/f noise at higher drive currents is partially balanced by the higher effective sensitivity of the sensor, and a customised optimisation of each individual sensor is often required.

Finally, the microstructure of the films can still be improved to achieve better figures of merit. A much higher Hall coefficient in films, evaporated at very high deposition rates was already found and high growth rates would also be expected to yield a finer-grained microstructure, leading to less current inhomogeneity and lower offset resistances. Without degrading the crystal structure or resistivity, it has recently been demonstrated that nanoscale mechanical polishing of Bi films deposited on oxidised Si substrates leads to much smoother films.[21] This approach could be used to optimise the figures of merit of Hall devices and may enable the manufacturing of even smaller sensors using advanced etching techniques.

CONCLUSIONS

The manufactured sensors reveal that the minimum detectable fields of our smallest devices are superior to those manufactured by FIB milling of continuous Bi-films. These sensors look very promising for applications in high resolution room temperature scanning Hall probe microscopy and a number of ways in which their performance could still be further explored.

REFERENCES

1. Martin, Y and Wickramasinghe, HK (1987). Magnetic imaging by ‘‘force microscopy’’with 1000 Å resolution. Applied Physics Letters, 1987; 50(20): 1455-1457.

2. Saenz, J; Garcia, N and Slonczewski, J. Theory of magnetic imaging by force microscopy. Applied physics letters, 1988; 53(15): 1449-1451.
3. Simon, J. Local magnetic probes of superconductors. Advances in Physics, 1999; 48(4): 449-535.
4. Novoselov, RS; Morozov, SV; Dubonos, SV, Missons, M and Volkov, AO. Sumicron probes for Hall mangetometry over the extended temprature range from helium to room temperature. Journal of Applied Physics, 2003; 93: 10053-10057.
5. Hicks, CW; Luan, L; Moler, KA; Zeldov, E and Shtrikman, H. Noise characteristics of 100 nm scale Ga As Al x Ga 1 x As scanning Hall probes; Appl. Phys. Lett, 2007 ; 90: 133512-3.
6. Vervaeke, K; Simoen, E; G Borghs, G and Moshchalkov, VV. Size dependence of microscopic Hall sensor detection limits. Review of Scientific Instruments, 2009; 80: 074701-1-7. American Institute of Physics. DOI: 10.1063/1.3160105
7. Gregory, JK; Bending, SJ and Sandhu, A. A scanning Hall probe microscope for large area magnetic imaging down to cryogenic temperatures. Review of Scientific Instruments, 2002; 73: 3515-3519. doi: 10.1063/1.150509.
8. Sandhu, A; Kurosawa, K; Dede, M and Oral, A. 50nm Hall Sensors for Room Temperature Scanning Hall Probe Microscopy, Japanese Journal of Applied Physics, 2004; 43(2): 777-778. DOI: 10.1143/JJAP.43.777.
9. Grigorenko AN; Bending, SJ; Gregory, JK and Humphreys, RG. Scanning Hall probe microscopy of flux penetration into a superconducting YBa2Cu3O7 thin film strip. Appl. Phys. Lett., 2001; 78: 1586-1588.
10. Kazakova, O; Gallop, JC; Cox, DC; Brown, E; Cuenat, A and Suzuki, K. "Optimization of 2DEG InAs/GaSb Hall Sensors for Single Particle Detection," in IEEE Transactions on Magnetics, 2008; 44(11): 4480-4483, doi: 10.1109/TMAG.2003507.
11. Pross, A; Crisan, AI; Bending, SJ; Mosser, V and Konczykowski, M. Second-generation quantum-well sensors for room-temperature scanning Hall probe microscopy, Journal of Applied Physics, 2005; 97: 096105-4. doi: 10.1063/1.1887828
12. Kazakova, O; Panchar, V, Callop, J; See, P; Cox, DC; Spasova, M and Cohen, LF. Ultrastructural particle detection using a submicron Hall sensor. Journal of Applied Physics, 2010; 107: 09E708-09E708-3. doi;10.1063/1.3360584.
13. Broom, RF and Rhoderick, EH. Studies of the Intermediate State in Thin Superconducting Films. Proc. Phys. Soc., 1962; 79: 586-593.
14. Goren, RN and Tinkham, M. Patterns of Magnetic Flux Penetration in Superconducting Films. J. Low Temp. Phys, 1971; 5(4): 465-494.
15. Petit, D; Atkinson, S; Johnston, D; Wood and R.P. Cowburn, RP. Room temperature performance of submicron bismuth Hall probes. IEE Proc.-Sci. Meas. Technol, 2004; 151: 127-130.
16. Petit, D; Faulkner, CC; Johnstone, S; Wood, D and Cowburn, RP. Nanometer scale patterning using focused ion beam milling. Review of Scientific Instruments, 2005; 76: 026105-3. doi: 10.1063/1.184443.
17. Kubota, M; Tokunaga, Y; Kanazawa, N; Kagawa, F; Tokura, Y and Kawasaki, M. Miniature Hall sensor integrated on a magnetic thin film for detecting domain wall motion. Journal of Applied Physics, 2013; 114: 053909-1-053909-4. doi: 10.1063/1.4817285.
18. Boffoue, MO; Lenoir, B; Jacquot, A; Scherrer, H; Dauscher, A; Stolzer, M. Structure and transport properties of polycrystalline Bi films, Journal of Physics and Chemistry of Solids, 2000; 61: 1979–1983. PII: S0022-3697(00)00186-4.
19. Hooge, F (1994). 1/f noise sources, IEEE Trans. Electr. Dev. 41(11): 1926-1935.
20. Hoffman, RA and Frankl, DR. Electrical Transport Properties of Thin Bismuth Films. Phys. Rev., 1971; 3: 1825-2. DOI:http://dx.doi.org/10.1103/PhysRevB.3.1825
21. Koseva, R; Mönch, I; Meier, D; Schumann, J; Arndt, KF; Schultz, L and Schmidt, OG. Evolution of hillocks in Bi-thin films and their removal upon nanoscale mechanical polishing, 2012; 520(17): 5589-5592. doi:10.1016/j.tsf.2012.04.040.